Benchmark solutions for the natural convective heat transfer problem in a square cavity with large horizontal temperature differences

Received October 2002
Revised March 2003
Accepted April 2003

Jan Vierendeels, Bart Merci and Erik Dick
Department of Flow, Heat and Combustion Mechanics, Ghent University, Ghent, Belgium

Keywords *Convection, Cavitation, Temperature distribution, Flow*

Abstract *In this study, Benchmark solutions are derived for the problem of two-dimensional laminar flow of air in a square cavity which is heated on the left, cooled on the right and insulated on the top and bottom boundaries. The temperature differences between the hot and cold walls are large. Neither Boussinesq nor low-Mach number approximations of the Navier-Stokes equations are used. The ideal-gas law is used and the viscosity is given by Sutherland's law. A constant Prandtl number is assumed. The computational method is completely described by Vierendeels et al. Grid converged results with an accuracy of 4 up to 5 digits are obtained for different Rayleigh numbers and temperature differences.*

Notations

C_p = specific heat capacity at constant pressure
g = gravitational constant
k = thermal conductivity
L = dimension of the cavity
Ma = Mach number
m = mass content in the cavity
Nu = Nusselt number
P = pressure
Pr = Prandtl number
R = specific gas constant
Ra = Rayleigh number
S = area of the cavity, temperature used in the Sutherland's law
T = temperature
u = velocity component in the x-direction
v = vecocity component in the y-direction
ε = non-dimensional temperature difference
γ = ratio of the specific heat capacities
μ = dynamic viscosity
Ψ = dimensionless stream function
ρ = density

Subscript

c = cold
h = hot
0 = reference

1. Definition of the problem

Flow of a compressible fluid is considered in a differentially heated square cavity in which large temperature differences are applied to the vertical walls while the horizontal walls are thermally insulated (Figure 1). This problem has

International Journal of Numerical Methods for Heat & Fluid Flow
Vol. 13 No. 8, 2003
pp. 1057-1078

0961-5539
DOI 10.1108/09615530310501957

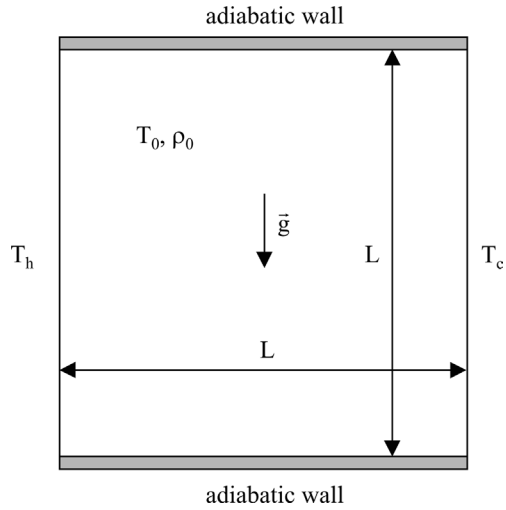

Figure 1.
Geometry, initial and boundary conditions for the thermally driven cavity problem

been studied by Chenoweth and Paolucci (1986) and Leonardi and Reizes (1981), but no benchmarking data are available from those studies.

The parameters defining the problem are: the dimension of the cavity L, the fluid properties R, $\mu(\mu^*, S, T^*)$, k, C_p and the specific buoyancy force $g\Delta\rho/\rho$. In contrast to the flows where the Boussinesq approximation is valid, the relative density variation also has a direct influence on the flowfield: it causes the divergence of the velocity field not to be zero anymore. With the use of ideal gas law, $\Delta\rho/\rho$ is defined by $\Delta T/T$ and $\Delta P/P$, so temperature and pressure differences and temperature and pressure levels become important parameters. The temperature difference and temperature level can be specified by the temperatures of the vertical walls, T_h and T_c. The pressure difference cannot be specified, but it is a solution of the problem, so this is not an independant parameter. The pressure level, however, is specified by the initial mass in the cavity m, the ideal gas law and the already specified temperature level and dimension of the cavity. The rank of the dimensional matrix is four, so there are seven dimensionless groups:

- The Prandtl number, $\mathrm{Pr} = \mu C_p/k$.
- The Rayleigh number, representing the driving force, defined for a compressible fluid as:

$$\mathrm{Ra} = \mathrm{Pr}\frac{g\rho_0^2(T_h - T_c)L^3}{T_0\mu_0^2},$$

where T_0 is the reference temperature equal to $(T_h + T_c)/2$, ρ_0 is the reference density corresponding to the initial mass in the cavity m and μ_0 is the reference dynamic viscosity, evaluated at T_0.

- The temperature difference may be represented by a non-dimensional parameter:

$$\varepsilon = \frac{T_h - T_c}{2T_0}. \quad (1)$$

  This parameter being part of the Rayleigh number has for non-Boussinesq flows its own significance: it represents the non-buoyancy influence of the temperature field on the flowfield. For small temperature differences ε reaches zero, which corresponds to the Boussinesq solution.
- Ma_{ref} and γ: These parameters describe the influence on the flowfield due to density changes from compressibility effects. Ma_{ref} is defined as v_{ref}/c_0, with v_{ref} a reference velocity and c_0, the speed of sound corresponding to T_0. An appropriate reference velocity v_{ref} can be derived from the Boussinesq solution for the natural convective heat transfer problem along a vertical wall: $v_{ref} = f(\mathrm{Pr})\mathrm{Ra}^{0.5}\mu(T_0)/(\rho_0 L)$ (White, 1974). Since in this paper only the solution for air is considered, the function $f(\mathrm{Pr})$ can be neglected, so the reference velocity becomes $v_{ref} = \mathrm{Ra}^{0.5}\mu(T_0)/(\rho_0 L)$. Since the reference Mach number is very small, both Ma_{ref} and γ have a negligible influence on the solution, but since the results are computed up to five digits, there may be an impact on the last digits. The Ma_{ref} number can be derived for each test case considered in this paper.
- S/T^* and T_0/T^*, defining the non-dimensional Sutherland's law.

The heat transfer through the wall is represented by local and average Nusselt numbers Nu and $\overline{\mathrm{Nu}}$:

$$\mathrm{Nu}(y) = \frac{L}{k_0(T_h - T_c)} k \left.\frac{\partial T}{\partial x}\right|_{wall},$$

$$\overline{\mathrm{Nu}} = \frac{1}{L}\int_{y=0}^{y=L} \mathrm{Nu}(y)\,\mathrm{d}y,$$

where $k = k(T)$ and $k_0 = k(T_0)$. In the test cases considered here, the Prandtl number is assumed to remain constant, equal to 0.71, and the dynamic viscosity is given by Sutherland's law:

$$\frac{\mu(T)}{\mu^*} = \left(\frac{T}{T^*}\right)^{3/2}\frac{T^* + S}{T + S}, \quad k(T) = \frac{\mu(T)C_p}{\mathrm{Pr}},$$

with $T^* = 273\,\mathrm{K}$, $S = 110.5\,\mathrm{K}$, $\mu^* = 1.68 \times 10^{-5}\,\mathrm{kg/m/s}$, $C_p = \gamma R/(\gamma - 1)$, $\gamma = 1.4$ and $R = 287.0\,\mathrm{J/kg/K}$. The influence of the temperature on C_p is neglected.

The problem is completely defined by the Rayleigh number, the value of ε, a reference state: $P_0 = 101,325\,\text{Pa}$, $T_0 = 600\,\text{K}$, $\rho_0 = P_0/(R\,T_0)$, the earlier mentioned fluid properties, dimension of the cavity $L = 1\,\text{m}$ and the initial mass content in the cavity, defined by ρ_0. During the computation, the mean pressure level is adjusted in order to keep the mass content constant.

2. Results

In the present study, six Rayleigh numbers, $\text{Ra} = 10^2$-10^7 are considered with a temperature difference parameter $\varepsilon = 0.6$. For the $\text{Ra} = 10^6$ case, calculations with $\varepsilon = 0.01, 0.2, 0.4$ and 0.6 are performed. Results are computed on a 1024×1024 stretched grid, of which the maximum aspect ratio is 80. Streamline patterns and temperature distributions are shown in Figures 2-4. Nusselt numbers and mean pressure values for the different Rayleigh numbers and ε are given in Tables I and II. The mean pressure is defined by

$$\bar{p} = \frac{1}{S}\int_S p\,\mathrm{d}S,$$

where S is the area of the cavity.

In Vierendeels *et al.* (2001), it was shown with the use of a 384×384, 512×512, 768×748 and 1024×1024 grid that quadratic grid convergence is obtained, that very good accuracy is obtained and that the computed results are correct up to four or five digits. It was also shown that the convergence behaviour is not influenced by the number of grid cells and grid aspect ratio.

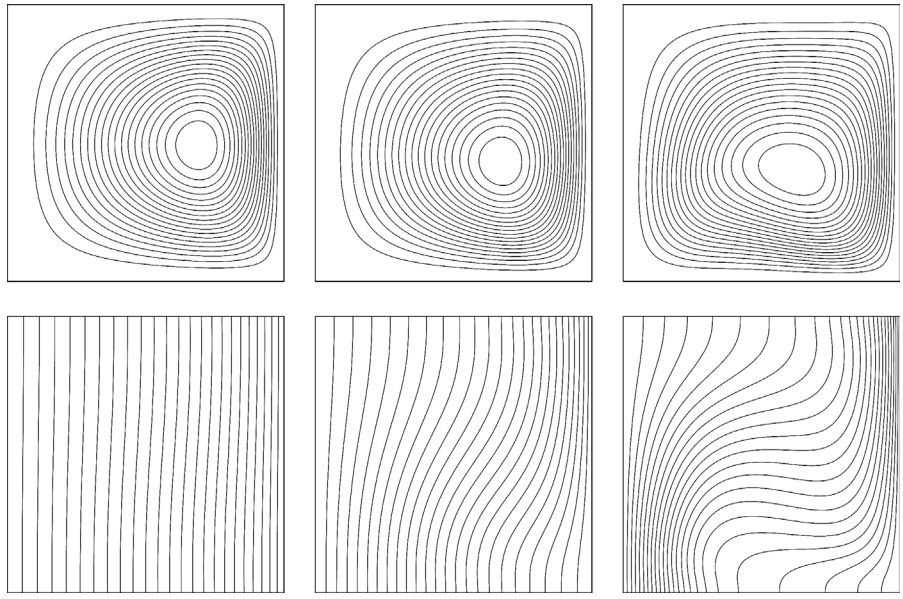

Figure 2.
Streamline patterns and temperature contours, $\varepsilon = 0.6$, $\text{Ra} = 10^2$-10^4

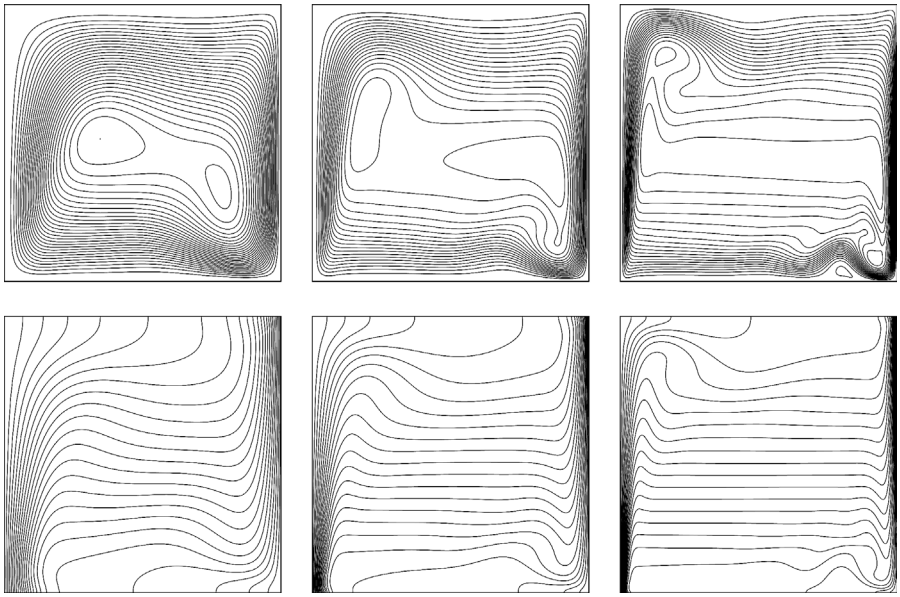

Figure 3.
Streamline patterns and temperature contours, $\varepsilon = 0.6$, $Ra = 10^5$-10^7

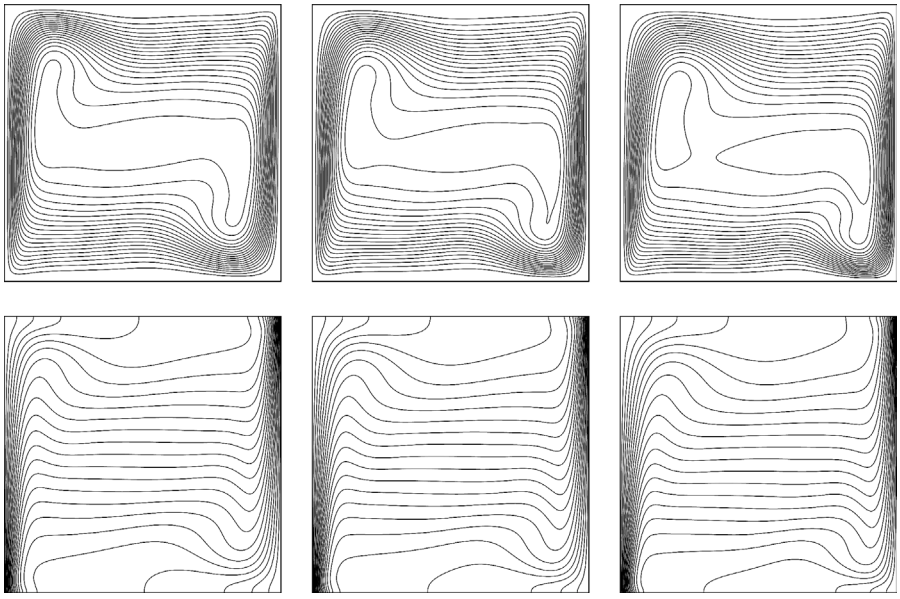

Figure 4.
Streamline patterns and temperature contours, $Ra = 10^6$, $\varepsilon = 0.01$, 0.2, 0.4

Nusselt number, velocity, temperature and reduced pressure, p_{reduced}, profiles at the walls and in the midplane are shown in Figures 5-13. Temperatures are made dimensionless by T_0, pressure by $\rho_0 v_{\text{ref}}^2$. The reduced pressure is given by:

$$p_{\text{reduced}} = p - \bar{p} + \rho_0 g(y - L/2).$$

Table III show computed values for different dimensionless parameters: the maximum and minimum Nusselt number and the Nusselt number at $y = 0.5$ are computed at left, mid and right position, the mean pressure, maximum Mach number, minimum and maximum velocity components at the mid planes, minimum and maximum divergence of the velocity and the stream function at the center and local minima and maxima of the stream function. The minima and maxima are computed using the quadratic reconstruction, because their positions do not necessarily coincide with the gridpoints.

3. Discussion

For $\varepsilon = 0.6$, there is a strong increase of the Nusselt number with the Rayleigh number. For the $\text{Ra} = 10^6$ case, there is a minor decrease of the Nusselt number with increasing ε values. For $\text{Ra} = 10^6$ and $\varepsilon = 0.01$, the Nusselt number corresponds with the calculation with Boussinesq approximation of Le Quéré (1991). The flowfield in this case is almost symmetrical, tending to the symmetrical Boussinesq solution. With increasing ε, the solution becomes more asymmetrical. The thickness of the boundary layers is hereby very slightly increasing corresponding to the very small decrease in Nusselt number. For a given $\varepsilon = 0.6$, however, there is a strong decrease in boundary layer thickness with increasing Rayleigh number, corresponding to the strong increase in Nusselt number. For the lowest Rayleigh numbers, the boundary

Table I.
Nusselt number and mean pressure for different Rayleigh numbers, and $\varepsilon = 0.6$

Ra	$\overline{\text{Nu}}$	$\bar{p}/P_0$
1E2	0.9787	0.95736
1E3	1.1077	0.93805
1E4	2.218	0.91463
1E5	4.480	0.92196
1E6	8.687	0.92449
1E7	16.241	0.92263

Table II.
Nusselt number and mean pressure for different values of ε, $\text{Ra} = 10^6$

ε	$\overline{\text{Nu}}$	$\bar{p}/P_0$
0.01	8.825	0.999998015
0.2	8.811	0.992009
0.4	8.768	0.96745
0.6	8.687	0.92449

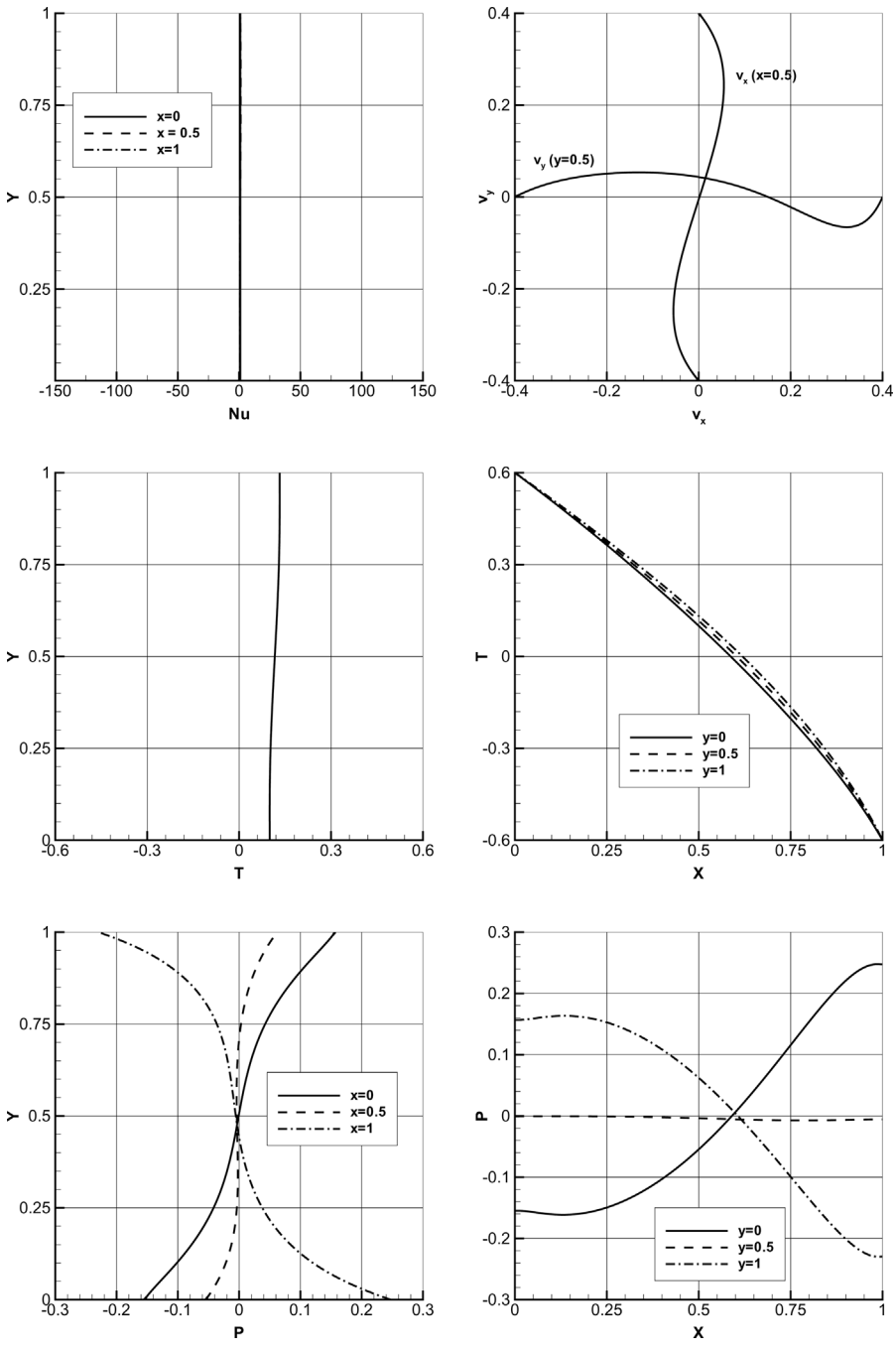

Figure 5.
Nusselt number profile in the vertical mid plane and velocity, temperature and reduced pressure profiles in both the mid planes, $Ra = 10^2$, and $\varepsilon = 0.6$

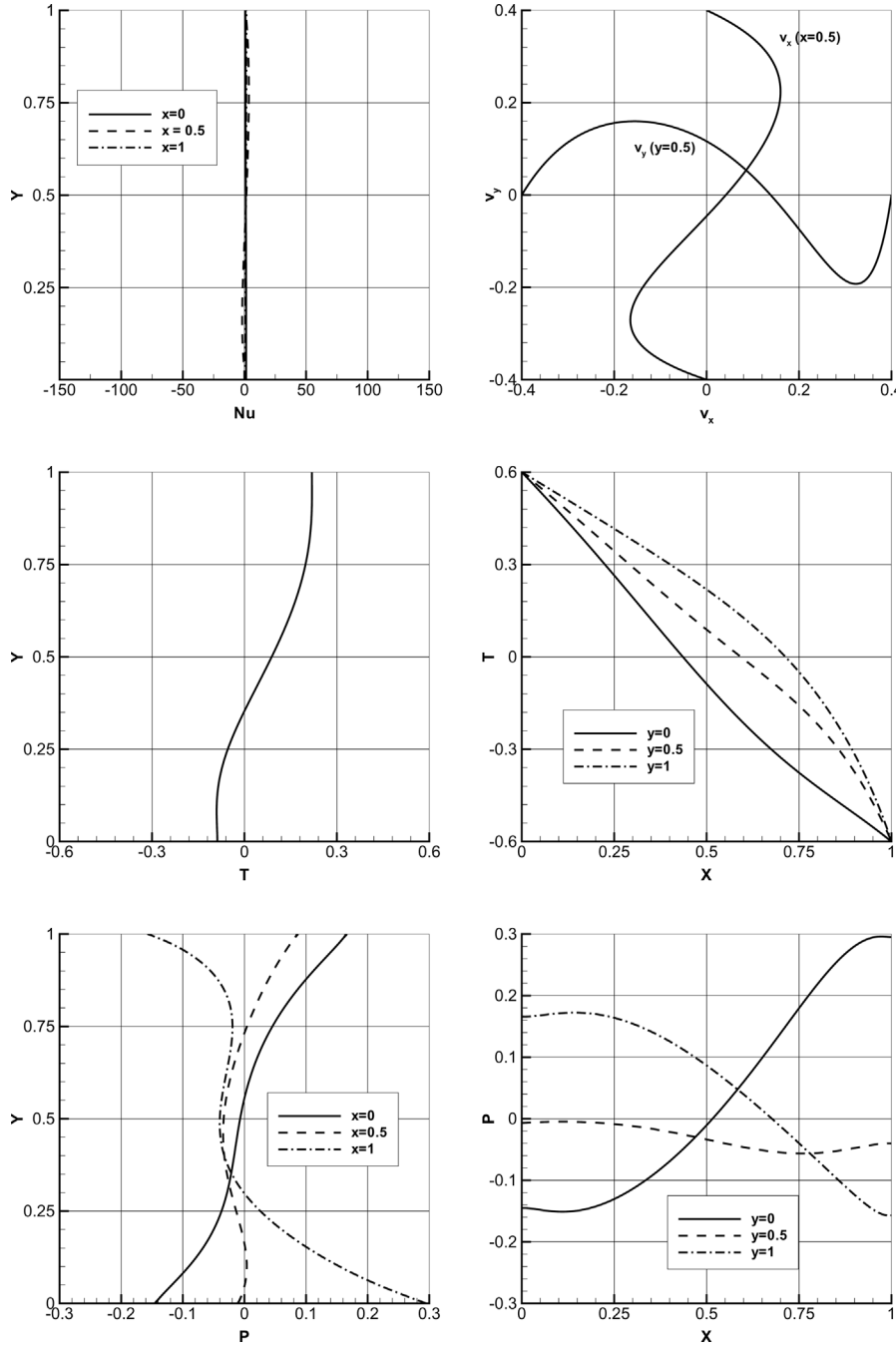

Figure 6.
Nusselt number profile in the vertical mid plane and velocity, temperature and reduced pressure profiles in both the mid planes, $Ra = 10^3$, and $\varepsilon = 0.6$

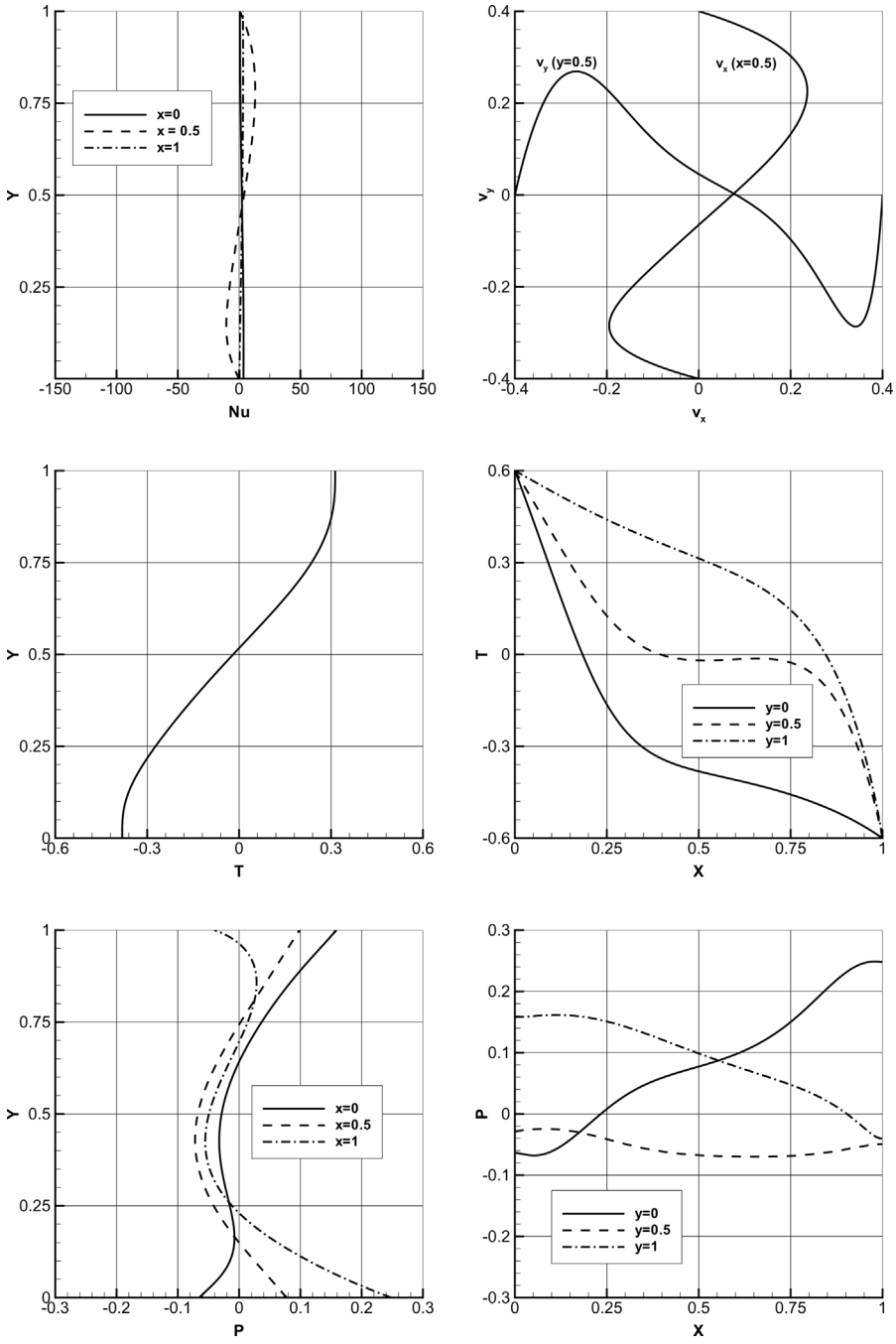

Figure 7.
Nusselt number profile in the vertical mid plane and velocity, temperature and reduced pressure profiles in both the mid planes, $Ra = 10^4$, and $\varepsilon = 0.6$

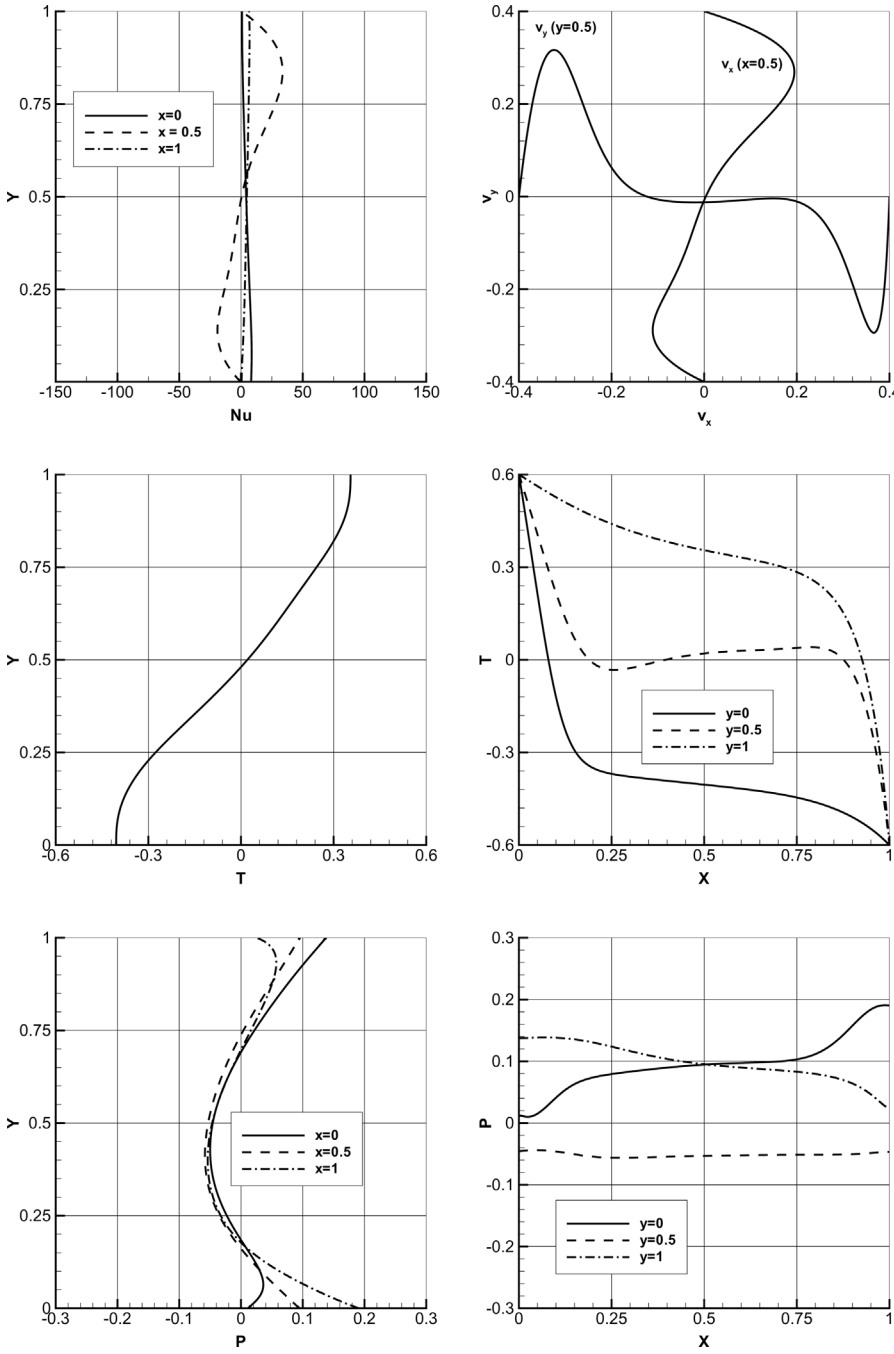

Figure 8.
Nusselt number profile in the vertical mid plane and velocity, temperature and reduced pressure profiles in both the mid planes, $Ra = 10^5$, and $\varepsilon = 0.6$

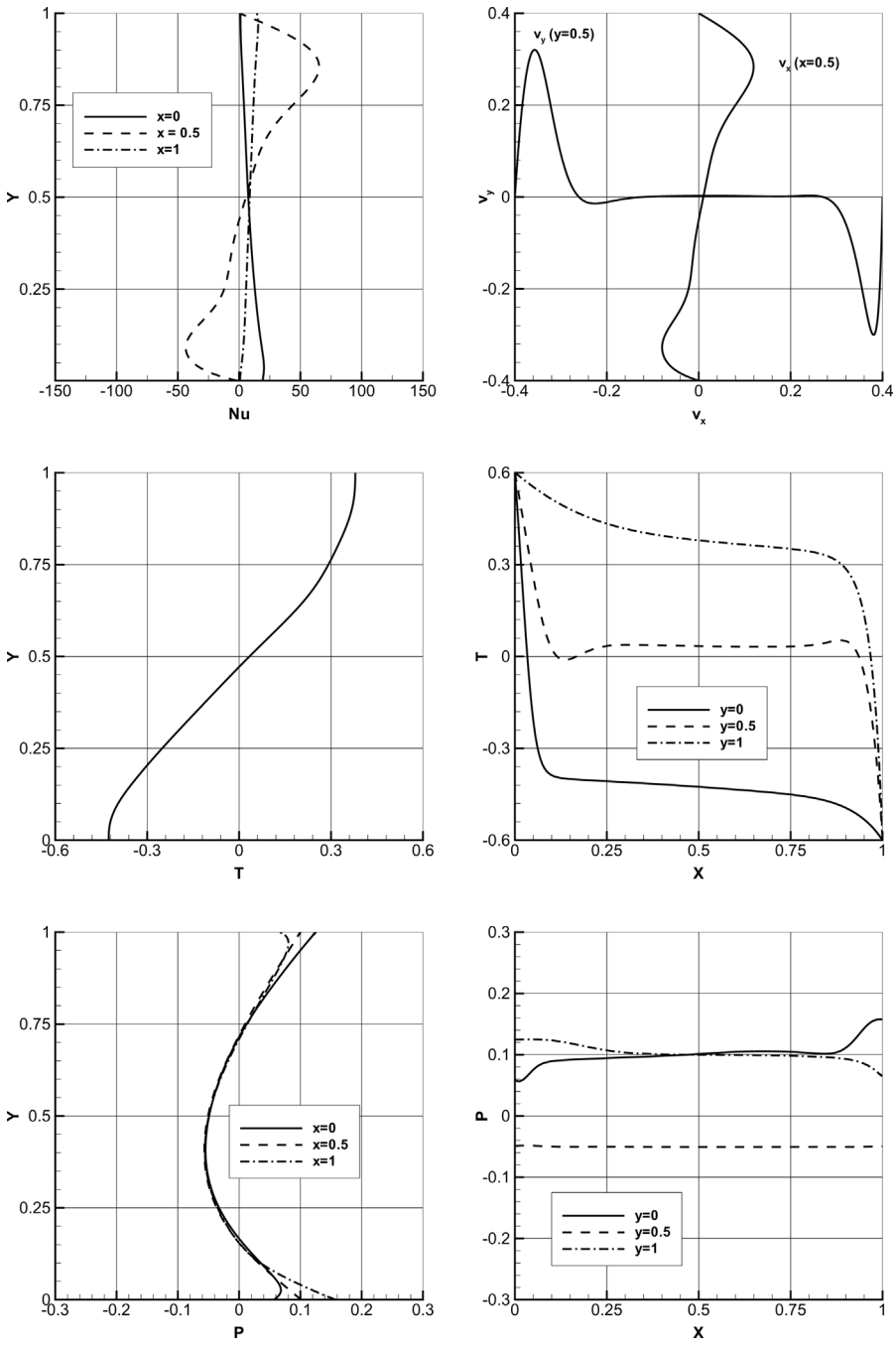

Figure 9.
Nusselt number profile in the vertical mid plane and velocity, temperature and reduced pressure profiles in both the mid planes, $Ra = 10^6$, and $\varepsilon = 0.6$

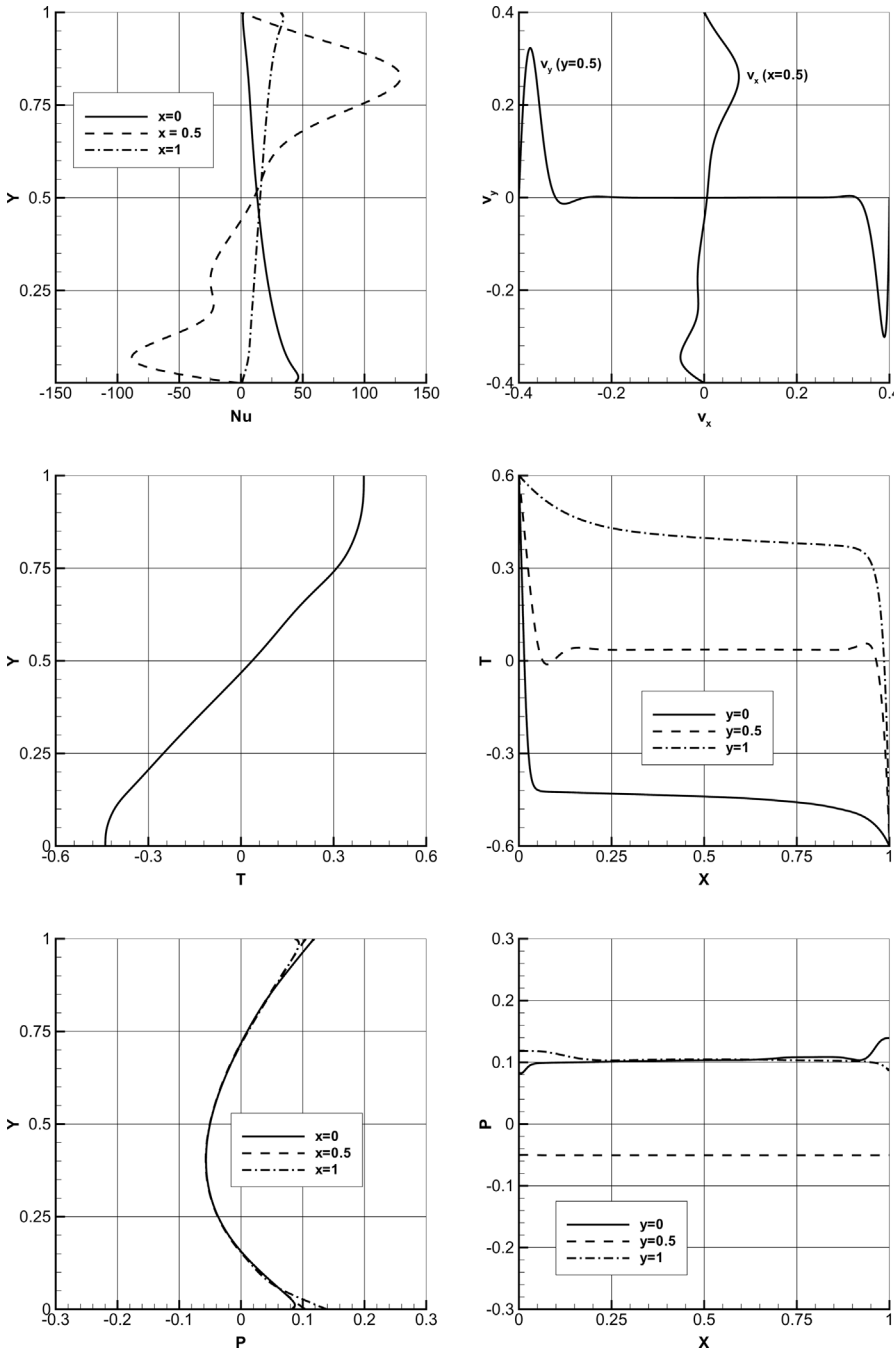

Figure 10.
Nusselt number profile in the vertical mid plane and velocity, temperature and reduced pressure profiles in both the mid planes, $Ra = 10^7$, and $\varepsilon = 0.6$

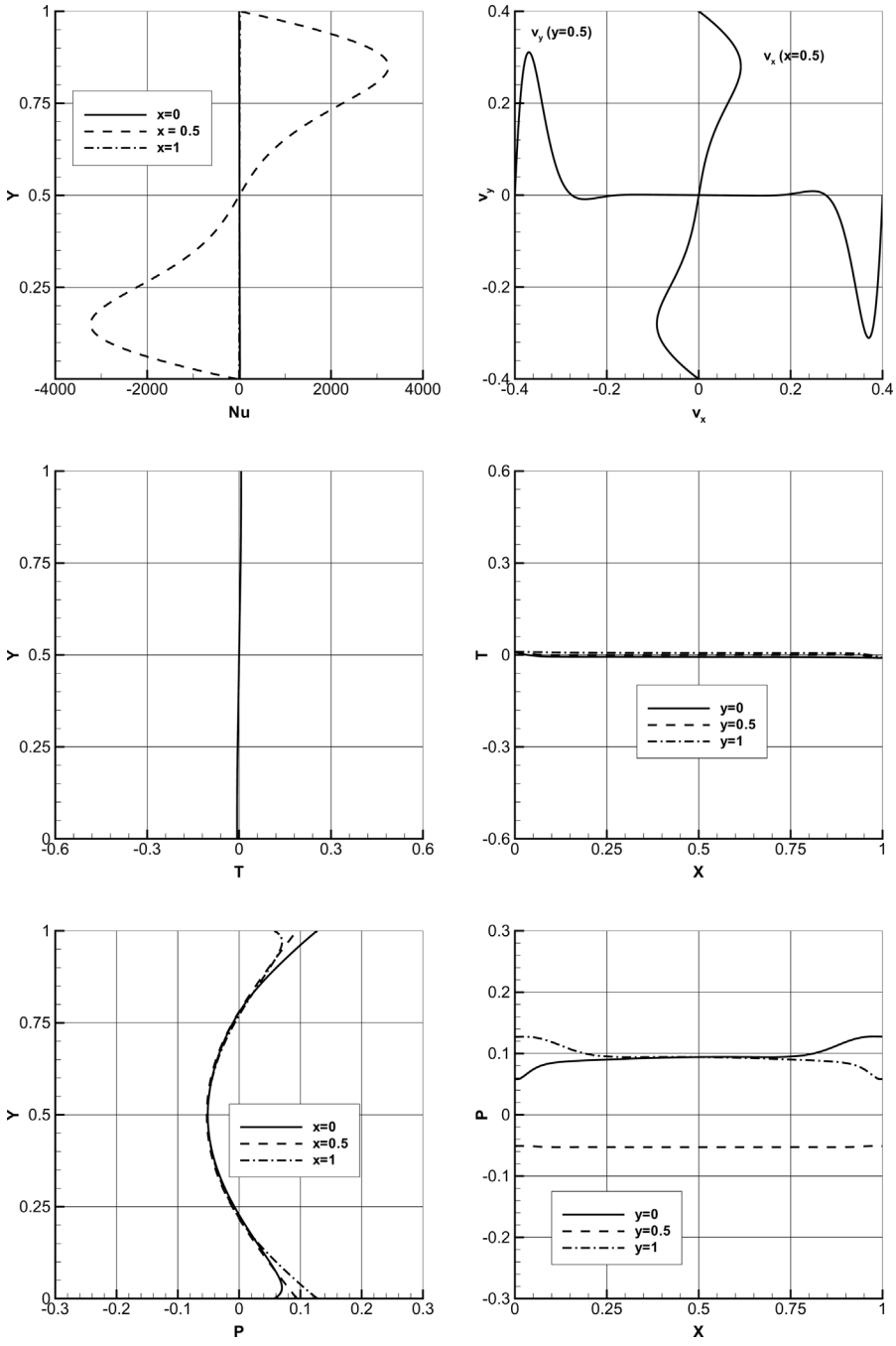

Figure 11.
Nusselt number profile in the vertical mid plane and velocity, temperature and reduced pressure profiles in both the mid planes, $Ra = 10^6$, and $\varepsilon = 0.01$

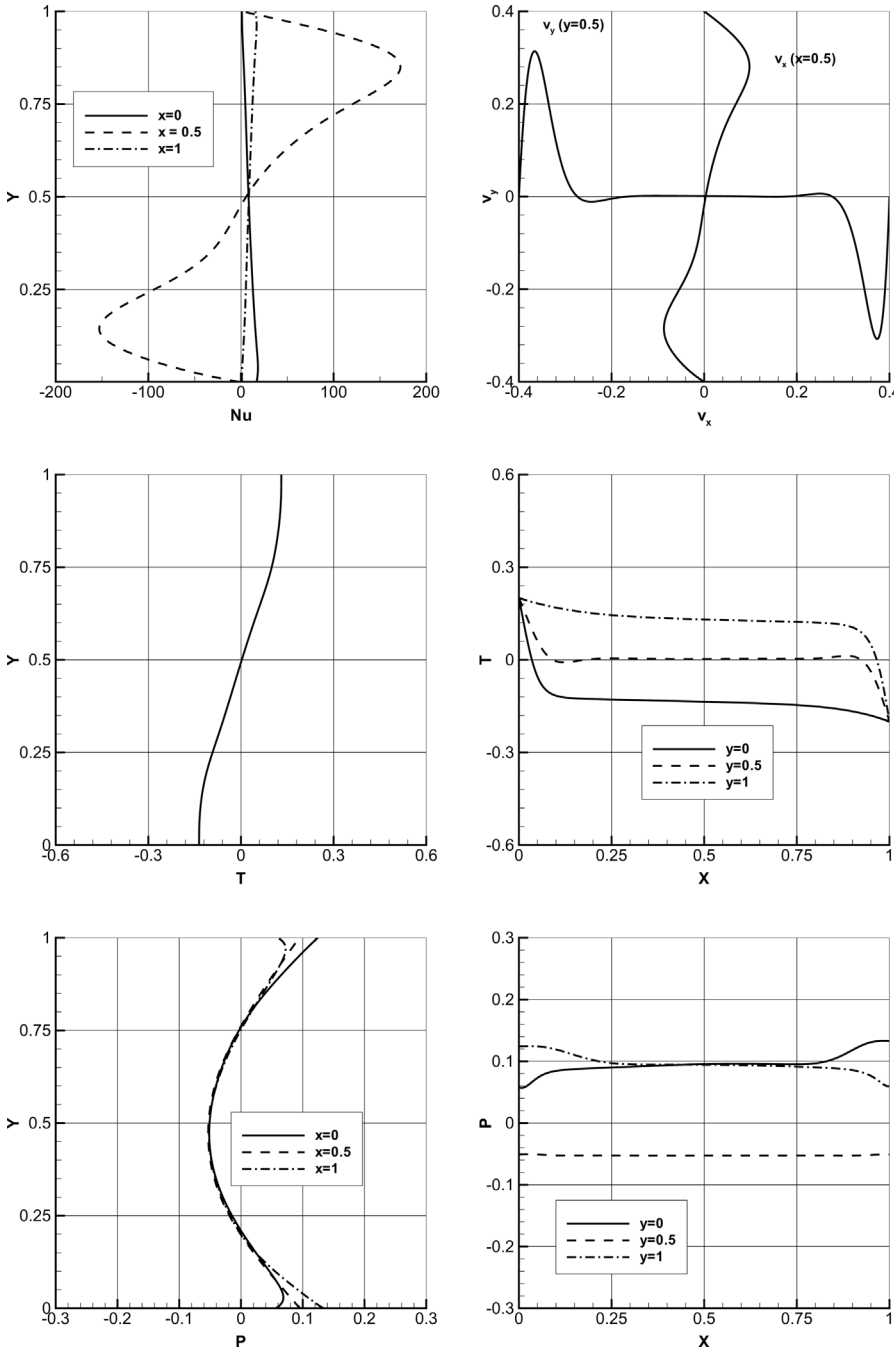

Figure 12.
Nusselt number profile in the vertical mid plane and velocity, temperature and reduced pressure profiles in both the mid planes, $Ra = 10^6$, and $\varepsilon = 0.2$

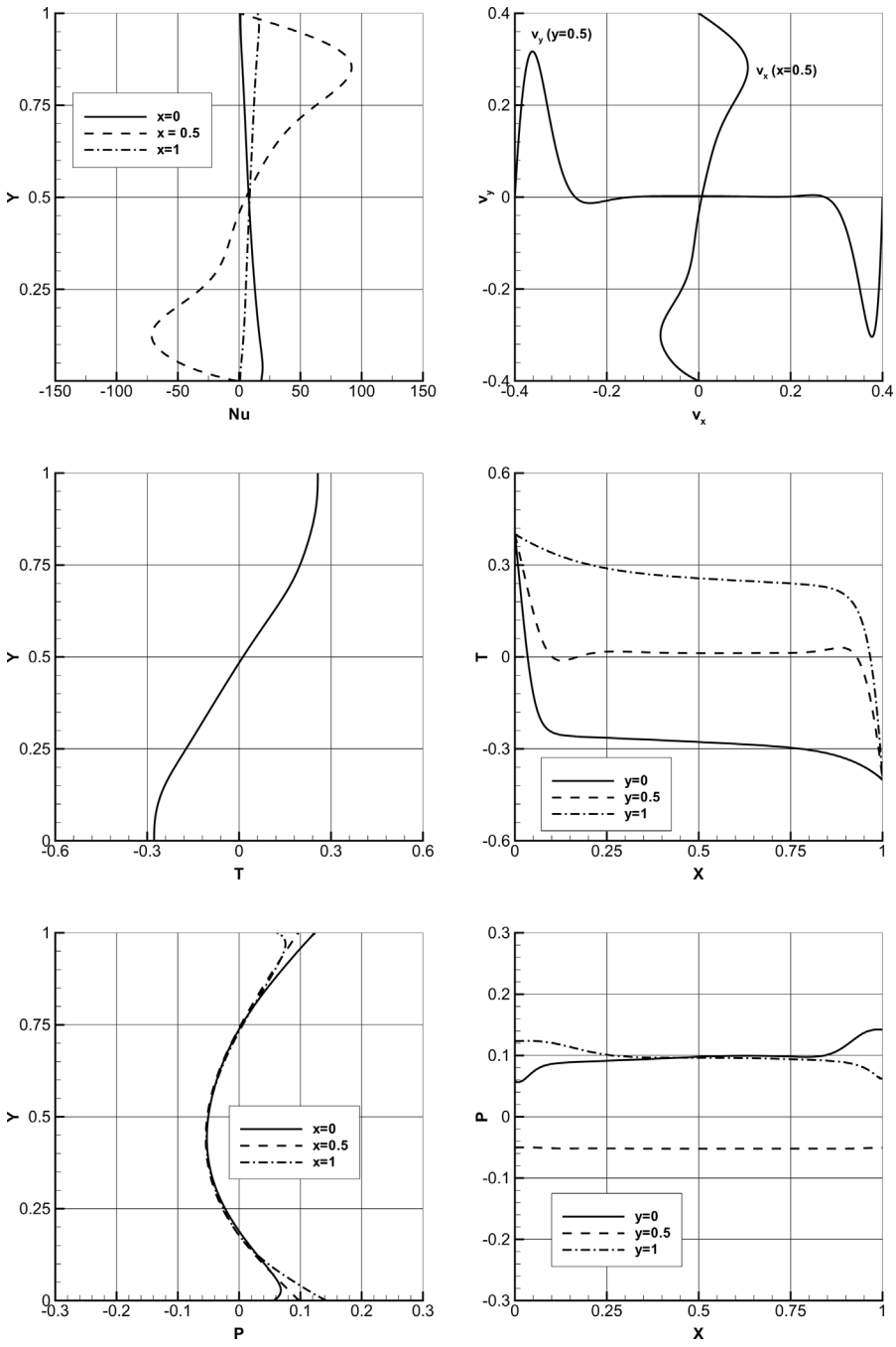

Figure 13.
Nusselt number profile in the vertical mid plane and velocity, temperature and reduced pressure profiles in both the mid planes, $Ra = 10^6$, and $\varepsilon = 0.4$

Variable	Value	Position
Computed values for $Ra = 10^2$ and $\varepsilon = 0.6$		
Right		
Nu_{max}	1.0509	(0.9101)
Nu_{min}	0.9034	(0.0755)
$\underline{Nu}_{mid}$	0.9804	(0.5)
$\overline{Nu}$	0.9787	–
Left		
Nu_{max}	1.0093	(0)
Nu_{min}	0.9481	(1)
$\underline{Nu}_{mid}$	0.9786	(0.5)
$\overline{Nu}$	0.9787	–
Mid		
Nu_{max}	1.2683	(0.8026)
$\underline{Nu}_{min}$	0.6831	(0.1911)
$\overline{Nu}$	0.9787	–
$\overline{Nu}_{conv}$	0.0024	–
$\overline{Nu}_{visc}$	0.9763	–
$\bar{p}/P_0$	0.95736	–
Ma_{max}	8.816×10^{-8}	(0.9145, 0.4940)
v_{max} $(y = 0.5)$	0.05347	(0.3367)
v_{min} $(y = 0.5)$	−0.06555	(0.9029)
u_{max} $(x = 0.5)$	0.05473	(0.8043)
u_{min} $(x = 0.5)$	−0.05509	(0.1890)
$(-\vec{v}/\rho \cdot \nabla\rho)_{max}$	0.08465	(0.7351, 0.1614)
$(\nabla \cdot \vec{v})_{max}$	0.08466	(0.7351, 0.1614)
$(-\vec{v}/\rho\nabla\rho)_{min}$	−0.08259	(0.7583, 0.8329)
$(\nabla \cdot \vec{v})_{min}$	−0.08260	(0.7583, 0.8329)
Ψ_{mid}	0.01515	(0.5, 0.5)
Ψ_{max_1}	0.01950	(0.6885, 0.4914)
Computed values for $Ra = 10^3$ and $\varepsilon = 0.6$		
Right		
Nu_{max}	1.6073	(0.8664)
Nu_{min}	0.4192	(0)
$\underline{Nu}_{mid}$	1.2019	(0.5)
$\overline{Nu}$	1.1077	–
Left		
Nu_{max}	1.4099	(0)
Nu_{min}	0.8052	(1)
$\underline{Nu}_{mid}$	1.1039	(0.5)
$\overline{Nu}$	1.1077	–
Mid		
Nu_{max}	3.602	(0.7800)
$\underline{Nu}_{min}$	−1.863	(0.1644)
$\overline{Nu}$	1.1077	–

(*continued*)

Table III.
Computed values for dimensionless parameters

Variable	Value	Position
$\overline{\mathrm{Nu}}_{\mathrm{conv}}$	0.2142	–
$\overline{\mathrm{Nu}}_{\mathrm{visc}}$	0.8936	–
$\bar{p}/P_0$	0.93805	–
$\mathrm{Ma}_{\max}$	8.078×10^{-7}	(0.9146, 0.4563)
$v_{\max}$ $(y = 0.5)$	0.1597	(0.3052)
$v_{\min}$ $(y = 0.5)$	−0.1926	(0.9036)
$u_{\max}$ $(x = 0.5)$	0.1599	(0.7801)
$u_{\min}$ $(x = 0.5)$	−0.1649	(0.1618)
$(-\vec{v}/\rho \cdot \nabla\rho)_{\max}$	0.2640	(0.5837, 0.1539)
$(\nabla \cdot \vec{v})_{\max}$	0.2640	(0.5838, 0.1539)
$(-\vec{v}/\rho\nabla\rho)_{\min}$	−0.2220	(0.8145, 0.8052)
$(\nabla \cdot \vec{v})_{\min}$	−0.2220	(0.8145, 0.8052)
Ψ_{mid}	0.04522	(0.5, 0.5)
$\Psi_{\max_1}$	0.05713	(0.6739, 0.4311)
Computed values for $Ra = 10^4$ and $\varepsilon = 0.6$		
Right		
$\mathrm{Nu}_{\max}$	3.282	(0.8497)
$\mathrm{Nu}_{\min}$	0.350	(0)
$\underline{\mathrm{Nu}}_{\mathrm{mid}}$	2.506	(0.5)
$\overline{\mathrm{Nu}}$	2.218	–
Left		
$\mathrm{Nu}_{\max}$	3.623	(0.1119)
$\mathrm{Nu}_{\min}$	0.758	(1)
$\underline{\mathrm{Nu}}_{\mathrm{mid}}$	2.202	(0.5)
$\overline{\mathrm{Nu}}$	2.218	–
Mid		
$\mathrm{Nu}_{\max}$	13.144	(0.7848)
$\underline{\mathrm{Nu}}_{\min}$	−10.460	(0.1460)
$\overline{\mathrm{Nu}}$	2.218	–
$\overline{\mathrm{Nu}}_{\mathrm{conv}}$	2.056	–
$\overline{\mathrm{Nu}}_{\mathrm{visc}}$	0.162	–
$\bar{p}/P_0$	0.91463	–
$\mathrm{Ma}_{\max}$	3.620×10^{-6}	(0.9365, 0.4211)
$v_{\max}$ $(y = 0.5)$	0.2688	(0.1666)
$v_{\min}$ $(y = 0.5)$	−0.2863	(0.9270)
$u_{\max}$ $(x = 0.5)$	0.2363	(0.7821)
$u_{\min}$ $(x = 0.5)$	−0.1948	(0.1444)
$(-\vec{v}/\rho \cdot \nabla\rho)_{\max}$	0.3945	(0.2080, 0.1396)
$(\nabla \cdot \vec{v})_{\max}$	0.3945	(0.2080, 0.1397)
$(-\vec{v}/\rho\nabla\rho)_{\min}$	−0.3001	(0.8938, 0.8363)
$(\nabla \cdot \vec{v})_{\min}$	−0.3001	(0.8938, 0.8364)
Ψ_{mid}	0.06472	(0.5, 0.5)
$\Psi_{\max_1}$	0.07060	(0.6229, 0.4013)

(*continued*)

Table III.

Variable	Value	Position
Computed values for $Ra = 10^5$ and $\varepsilon = 0.6$		
Right		
Nu_{max}	6.933	(0.9314)
Nu_{min}	0.515	(0)
$\underline{Nu}_{mid}$	4.740	(0.5)
$\overline{Nu}$	4.480	–
Left		
Nu_{max}	8.641	(0.0754)
Nu_{min}	0.848	(1)
$\underline{Nu}_{mid}$	4.203	(0.5)
$\overline{Nu}$	4.480	–
Mid		
Nu_{max}	33.65	(0.8375)
$\underline{Nu}_{min}$	−19.10	(0.1394)
$\overline{Nu}$	4.480	–
$\overline{Nu}_{conv}$	4.474	–
$\overline{Nu}_{visc}$	0.006	–
$\bar{p}/P_0$	0.92196	–
Ma_{max}	1.174×10^{-5}	(0.9632, 0.3644)
v_{max} $(y = 0.5)$	0.3166	(0.0948)
v_{min} $(y = 0.5)$	−0.2939	(0.9578)
u_{max} $(x = 0.5)$	0.1946	(0.8364)
u_{min} $(x = 0.5)$	−0.1111	(0.1394)
$(-\vec{v}/\rho \cdot \nabla\rho)_{max}$	0.6239	(0.0874, 0.0686)
$(\nabla \cdot \vec{v})_{max}$	0.6238	(0.0874, 0.0686)
$(-\vec{v}/\rho\nabla\rho)_{min}$	−0.4012	(0.9558, 0.9497)
$(\nabla \cdot \vec{v})_{min}$	−0.4012	(0.9558, 0.9497)
Ψ_{mid}	0.04092	(0.5, 0.5)
Ψ_{max_1}	0.04232	(0.3481, 0.5151)
Ψ_{max_2}	0.04135	(0.7846, 0.3349)
Computed values for $Ra = 10^6$ and $\varepsilon = 0.6$		
Right		
Nu_{max}	15.519	(0.9676)
Nu_{min}	0.758	(0)
$\underline{Nu}_{mid}$	8.637	(0.5)
$\overline{Nu}$	8.687	–
Left		
Nu_{max}	20.270	(0.0365)
Nu_{min}	1.067	(1)
$\underline{Nu}_{mid}$	7.459	(0.5)
$\overline{Nu}$	8.687	–
Mid		
Nu_{max}	65.23	(0.8544)
Nu_{min}	−43.56	(0.0905)

Table III. (*continued*)

Variable	Value	Position
$\overline{\mathrm{Nu}}$	8.687	–
$\overline{\mathrm{Nu}}_{\mathrm{conv}}$	8.690	–
$\overline{\mathrm{Nu}}_{\mathrm{visc}}$	−0.004	–
$\bar{p}/P_0$	0.92449	–
$\mathrm{Ma}_{\max}$	3.720×10^{-5}	(0.9792, 0.3787)
$v_{\max}$ $(y = 0.5)$	0.3203	(0.0537)
$v_{\min}$ $(y = 0.5)$	−0.3001	(0.9756)
$u_{\max}$ $(x = 0.5)$	0.1193	(0.8541)
$u_{\min}$ $(x = 0.5)$	−0.07972	(0.0905)
$(-\vec{v}/\rho \cdot \nabla\rho)_{\max}$	1.0394	(0.0384, 0.0303)
$(\nabla \cdot \vec{v})_{\max}$	1.0393	(0.0384, 0.0303)
$(-\vec{v}/\rho\nabla\rho)_{\min}$	−0.6086	(0.9794, 0.9762)
$(\nabla \cdot \vec{v})_{\min}$	−0.6086	(0.9794, 0.9762)
Ψ_{mid}	0.02209	(0.5, 0.5)
$\Psi_{\max_1}$	0.02351	(0.8688, 0.3926)
$\Psi_{\max_2}$	0.02312	(0.2081, 0.6477)
$\Psi_{\max_3}$	0.02126	(0.8880, 0.1458)
Computed values for $Ra = 10^7$ and $\varepsilon = 0.6$		
Right		
$\mathrm{Nu}_{\max}$	34.269	(0.9848)
$\mathrm{Nu}_{\min}$	1.089	(0)
$\overline{\mathrm{Nu}}_{\mathrm{mid}}$	15.512	(0.5)
$\overline{\mathrm{Nu}}$	16.240	–
Left		
$\mathrm{Nu}_{\max}$	46.379	(0.0164)
$\mathrm{Nu}_{\min}$	1.454	(1)
$\overline{\mathrm{Nu}}_{\mathrm{mid}}$	13.188	(0.5)
$\overline{\mathrm{Nu}}$	16.241	–
Mid		
$\mathrm{Nu}_{\max}$	129.35	(0.8260)
$\overline{\mathrm{Nu}}_{\min}$	−88.43	(0.0693)
$\overline{\mathrm{Nu}}$	16.241	–
$\overline{\mathrm{Nu}}_{\mathrm{conv}}$	16.205	–
$\overline{\mathrm{Nu}}_{\mathrm{visc}}$	0.036	–
$\bar{p}/P_0$	0.92263	–
$\mathrm{Ma}_{\max}$	1.175×10^{-4}	(0.9883, 0.3754)
$v_{\max}$ $(y = 0.5)$	0.3229	(0.0305)
$v_{\min}$ $(y = 0.5)$	−0.3011	(0.9861)
$u_{\max}$ $(x = 0.5)$	0.07490	(0.8260)
$u_{\min}$ $(x = 0.5)$	−0.05124	(0.0693)
$(-\vec{v}/\rho \cdot \nabla\rho)_{\max}$	1.7061	(0.0172, 0.0134)
$(\nabla \cdot \vec{v})_{\max}$	1.7058	(0.0172, 0.0134)
$(-\vec{v}/\rho\nabla\rho)_{\min}$	−0.9051	(0.9903, 0.9888)
$(\nabla \cdot \vec{v})_{\min}$	−0.9052	(0.9903, 0.9888)

(*continued*)

Table III.

Variable	Value	Position
Ψ_{mid}	0.01265	(0.5, 0.5)
Ψ_{max_1}	0.01315	(0.0989, 0.5016)
Ψ_{max_2}	0.01211	(0.1639, 0.8211)
Ψ_{max_3}	0.01282	(0.2798, 0.4556)
Ψ_{max_4}	−0.00013	(0.8009, 0.0419)
Ψ_{max_5}	0.01288	(0.8040, 0.4301)
Ψ_{max_6}	0.00922	(0.8807, 0.1765)
Ψ_{max_7}	0.01104	(0.9207, 0.0793)
Ψ_{max_8}	0.01324	(0.9256, 0.3909)
Computed values for $Ra = 10^6$ and $\varepsilon = 0.01$		
Right		
Nu_{max}	17.501	(0.9608)
Nu_{min}	0.977	(0)
$\overline{Nu}_{mid}$	8.389	(0.5)
$\overline{Nu}$	8.825	–
Left		
Nu_{max}	17.571	(0.0392)
Nu_{min}	0.982	(1)
$\overline{Nu}_{mid}$	8.370	(0.5)
$\overline{Nu}$	8.825	–
Mid		
Nu_{max}	3251	(0.8499)
$\overline{Nu}_{min}$	−3232	(0.1500)
$\overline{Nu}$	8.825	–
$\overline{Nu}_{conv}$	8.773	–
$\overline{Nu}_{visc}$	0.052	–
$\bar{p}/P_0$	0.99998015	–
Ma_{max}	3.189×10^{-5}	(0.9635, 0.5286)
v_{max} $(y = 0.5)$	0.3108	(0.0380)
v_{min} $(y = 0.5)$	−0.3105	(0.9625)
u_{max} $(x = 0.5)$	0.09158	(0.8499)
u_{min} $(x = 0.5)$	−0.09106	(0.1500)
$(-\vec{v}/\rho \cdot \nabla\rho)_{max}$	0.01123	(0.0325, 0.0315)
$(\nabla \cdot \vec{v})_{max}$	0.01112	(0.0324, 0.0319)
$(-\vec{v}/\rho\nabla\rho)_{min}$	−0.01114	(0.9678, 0.9686)
$(\nabla \cdot \vec{v})_{min}$	−0.01124	(0.9677, 0.9690)
Ψ_{mid}	0.02308	(0.5, 0.5)
Ψ_{max_1}	0.02367	(0.1507, 0.5461)
Ψ_{max_2}	0.02308	(0.5122, 0.5003)
Ψ_{max_3}	0.02368	(0.8499, 0.4527)
Computed values for $Ra = 10^6$ and $\varepsilon = 0.2$		
Right		
Nu_{max}	16.864	(0.9619)
Nu_{min}	0.927	(0)

Table III. (*continued*)

Variable	Value	Position
$\underline{\mathrm{Nu}}_{\mathrm{mid}}$	8.536	(0.5)
$\overline{\mathrm{Nu}}$	8.811	–
Left		
$\mathrm{Nu}_{\mathrm{max}}$	18.280	(0.0394)
$\mathrm{Nu}_{\mathrm{min}}$	1.019	(1)
$\underline{\mathrm{Nu}}_{\mathrm{mid}}$	8.154	(0.5)
$\overline{\mathrm{Nu}}$	8.811	–
Mid		
$\mathrm{Nu}_{\mathrm{max}}$	172.10	(0.8504)
$\underline{\mathrm{Nu}}_{\mathrm{min}}$	−152.99	(0.1439)
$\overline{\mathrm{Nu}}$	8.811	–
$\overline{\mathrm{Nu}}_{\mathrm{conv}}$	8.766	–
$\overline{\mathrm{Nu}}_{\mathrm{visc}}$	0.045	–
$\bar{p}/P_0$	0.992009	–
$\mathrm{Ma}_{\mathrm{max}}$	3.284×10^{-5}	(0.9679, 0.4874)
v_{max} $(y = 0.5)$	0.3138	(0.04246)
v_{min} $(y = 0.5)$	−0.3074	(0.9667)
u_{max} $(x = 0.5)$	0.09773	(0.8504)
u_{min} $(x = 0.5)$	−0.08694	(0.1440)
$(-\vec{v}/\rho \cdot \nabla\rho)_{\mathrm{max}}$	0.2469	(0.0349, 0.0320)
$(\nabla \cdot \vec{v})_{\mathrm{max}}$	0.2468	(0.0349, 0.0320)
$(-\vec{v}/\rho\nabla\rho)_{\mathrm{min}}$	−0.2096	(0.9708, 0.9700)
$(\nabla \cdot \vec{v})_{\mathrm{min}}$	−0.2097	(0.9708, 0.9700)
Ψ_{mid}	0.02295	(0.5, 0.5)
Ψ_{max_1}	0.02354	(0.1570, 0.5365)
Ψ_{max_2}	0.02308	(0.6366, 0.4902)
Ψ_{max_3}	0.02373	(0.8555, 0.4385)
Computed values for $Ra = 10^6$ *and* $\varepsilon = 0.4$		
Right		
$\mathrm{Nu}_{\mathrm{max}}$	16.208	(0.9642)
$\mathrm{Nu}_{\mathrm{min}}$	0.857	(0)
$\underline{\mathrm{Nu}}_{\mathrm{mid}}$	8.627	(0.5)
$\overline{\mathrm{Nu}}$	8.768	–
Left		
$\mathrm{Nu}_{\mathrm{max}}$	19.166	(0.0385)
$\mathrm{Nu}_{\mathrm{min}}$	1.048	(1)
$\underline{\mathrm{Nu}}_{\mathrm{mid}}$	7.851	(0.5)
$\overline{\mathrm{Nu}}$	8.768	–
Mid		
$\mathrm{Nu}_{\mathrm{max}}$	91.84	(0.8526)
$\underline{\mathrm{Nu}}_{\mathrm{min}}$	−71.35	(0.1248)
$\overline{\mathrm{Nu}}$	8.768	–
$\overline{\mathrm{Nu}}_{\mathrm{conv}}$	8.743	–
$\overline{\mathrm{Nu}}_{\mathrm{visc}}$	0.025	–

(*continued*)

Table III.

Variable	Value	Position
$\bar{p}/P_0$	0.96745	–
$\mathrm{Ma}_{\max}$	3.450×10^{-5}	(0.9731, 0.4387)
$v_{\max}$ $(y = 0.5)$	0.3170	(0.0477)
$v_{\min}$ $(y = 0.5)$	−0.3040	(0.9711)
$u_{\max}$ $(x = 0.5)$	0.1070	(0.8525)
$u_{\min}$ $(x = 0.5)$	−0.08322	(0.1248)
$(-\vec{v}/\rho \cdot \nabla\rho)_{\max}$	0.5690	(0.0370, 0.0316)
$(\nabla \cdot \vec{v})_{\max}$	0.5689	(0.0370, 0.0316)
$(-\vec{v}/\rho\nabla\rho)_{\min}$	−0.4054	(0.9746, 0.9724)
$(\nabla \cdot \vec{v})_{\min}$	−0.4055	(0.9746, 0.9724)
Ψ_{mid}	0.02261	(0.5, 0.5)
$\Psi_{\max_1}$	0.02335	(0.1658, 0.5319)
$\Psi_{\max_2}$	0.02320	(0.1888, 0.6669)
$\Psi_{\max_3}$	0.02320	(0.1878, 0.6637)
$\Psi_{\max_4}$	0.02369	(0.8616, 0.4187)
$\Psi_{\max_5}$	0.02201	(0.8691, 0.1855)

Table III.

layer fills the whole domain. For higher Rayleigh number separate boundary layers on the hot and cold wall can be detected. For low Rayleigh numbers the stream function shows only one local maximum. For higher Rayleigh numbers more local maxima are present. The accurate positions of these maxima can be found in the tables. For the $\mathrm{Ra} = 10^7$, $\varepsilon = 0.6$ case, even a minimum can be found, corresponding to a counterrotating vortex.

Additional physical discussions on the flow phenomena can be found in Chenoweth and Paolucci (1986) and Leonardi and Reizes (1981), but are not the attemption of this benchmark paper.

4. Conclusion

Benchmark solutions for different Ra-numbers and temperature differences ε for the square cavity problem with large temperature differences between the vertical planes are presented with an accuracy of four up to five digits.

References

Chenoweth, D.R. and Paolucci, S. (1986), "Natural convection in an enclosed vertical air layer with large horizontal temperature differences", *Journal of Fluid Mechanics*, Vol. 169, pp. 173-2105.

Leonardi, E. and Reizes, J.A. (1981), "Convective flows in closed cavities with variable fluid properties", in Lewis, R.W., Morgan, K. and Zienkiewicz, O.C. (Eds), *Numerical Methods in Heat Transfer*, Wiley, NY, pp. 387-412.

Le Quéré, P. (1991), "Accurate solutions to the square thermally driven cavity at high Rayleigh number", *Computers Fluids*, Vol. 20, pp. 29-41.

Vierendeels, J., Merci, B. and Dick, E. (2001), "Numerical study of natural convective heat transfer with large temperature differences", *International Journal of Numerical Methods for Heat and Fluid Flow*, Vol. 11, pp. 329-41.

White, F.M. (1974), *Viscous Fluid Flow*, McGraw-Hill, NY ISBN 007-069712-4.